



MET.O.11 TECHNICAL NOTE No. 41

A semi-implicit reformulation of the
Bushby-Timpson 10-level model

by

D. M. BURRIDGE

NB. This paper has not been published. Permission to quote from it should be
obtained from the Assistant Director of the above Meteorological Office Branch.

JUNE 1973

-No-

RETAIN THIS MASTER FOR FURTHER REPRODUCTION

Meteorological Office

4433

1. Introduction

Numerical weather prediction with the primitive equations is now a routine procedure in meteorological offices and services in many countries, and considerable effort has been and is being expended on developing efficient time-stepping schemes to enable the computations to be performed quickly enough to be useful within an operational environment. The most commonly used schemes are explicit; these are non-iterative 'marching' processes for obtaining the solution at each point in space at which dependent variables are kept at a new time level in terms of known values at earlier time-levels. Two of the most well known of these schemes are the leap-frog, or centred schemes, and the Lax-Wendroff two-step scheme, with the horizontal grid staggered in both space and time as suggested by Eliassen (1956) and used by Bushby and Timpson (1967). Explicit schemes for the primitive equations are subject to severe stability criteria which restrict the time-step, τ , that can be used. For the leap-frog scheme we must have $\tau < 2^{-1/2} \Delta X / (|C_g| + |V|_{\max})$ for stability, whilst for the Lax-Wendroff two-step scheme we require $\tau < 2^{-1/2} \Delta X / (C_g^2 + V_{\max}^2)^{1/2}$, C_g is the speed of the external gravity wave in the model, V is the meteorological wind and ΔX is the horizontal grid length. Since $C_g \approx 300 \text{ ms}^{-1}$ and V rarely exceeds 100 ms^{-1} these criteria are dominated by the speed of the gravity waves and allow a maximum time-step of about 3 minutes with $\Delta X = 100 \text{ km}$. Earlier and more simplified models, for example Bushby and Whitelam (1961), used a quasi-nondivergent approximation which eliminates the gravity waves entirely from the system so that stability depends only on the wind speed, with a time-step restriction of the form $\tau < \Delta X / (\sqrt{2} |V|_{\max})$. Robert et al (1972) developed a semi-implicit method which is subject to the same stability criterion. Both these methods involve the solution of three-dimensional Helmholtz equations or equivalently systems of coupled two-dimensional Helmholtz equations,

the number of two-dimensional equations being equal to the number of levels at which the dependent variables are kept in the vertical.

Since it is the presence of gravity waves in the model that governs the maximum allowable time-step a study was made of the solutions of a simplified form of the primitive equations that only describe the motion of pure gravity waves. This study led to the development of a semi-implicit reformulation of the Bushby-Timpson (1967) 10-level model which requires the solution of only two uncoupled Helmholtz equations.

In section 2. a brief description is given of the 10-level model. Section 3 gives the equations for pure gravity waves in the 10-level model and describes the properties of their solutions and also presents implicit and explicit integration schemes for these equations. The semi-implicit algorithm for the models primitive equations is described in section 4 and a short discussion of the progress with the scheme is given in section 5.

2. The governing equations

The horizontal co-ordinates (X, Y) are taken on a stereographic map projection with the origin at the North Pole; the hydrostatic pressure p is the vertical co-ordinate. The vertical resolution is 100mb, the model atmosphere being bounded by the 1000mb and 100mb surfaces. Horizontal components of velocity $u (= dx/dt)$ and $v (= dy/dt)$ are used to define the motion on the pressure surfaces $p = 1000\text{mb}, 900\text{mb}, \dots, 100\text{mb}$ the vertical velocity $\omega (= dp/dt)$ being kept at the nine levels midway between these pressure surfaces and at 1000mb. A diagram showing the arrangement of variables in the vertical is given in Figure 1.

The equations of motion are

$$\frac{\partial u^*}{\partial t} + \mu \left(u^* \frac{\partial u^*}{\partial x} + v^* \frac{\partial u^*}{\partial y} \right) + \omega \frac{\partial u^*}{\partial p} + \frac{1}{2} (u^{*2} + v^{*2}) \frac{\partial \mu}{\partial x} + g \frac{\partial h}{\partial x} - f v^* = F_x \quad (1)$$

$$\frac{\partial v^*}{\partial t} + \mu \left(u^* \frac{\partial v^*}{\partial x} + v^* \frac{\partial v^*}{\partial y} \right) + \omega \frac{\partial v^*}{\partial p} + \frac{1}{2} (u^{*2} + v^{*2}) \frac{\partial \mu}{\partial y} + g \frac{\partial h}{\partial y} + f u^* = F_y \quad (2)$$

for each of the ten pressure levels of the model, h is the height of the pressure surface, $u^* = u/m$, $v^* = v/m$, $\mu = m^2$, f the coriolis parameter, $m (= \sec^2(\pi/4 - \phi/2))$, ϕ being the latitude) is the map magnification factor and g the acceleration due to gravity. The functions F_x and F_y represent the frictional and horizontal diffusion terms.

The equation of continuity is used in the form

$$\mu \left(\frac{\partial u^*}{\partial x} + \frac{\partial v^*}{\partial y} \right) + \frac{\partial \omega}{\partial p} = 0 \quad (3)$$

The integration of this equation with respect to pressure is discussed below.

The thermodynamic equation expressed in terms of 100mb layer thicknesses

h' , h' is proportional to the mean temperature of that 100mb slab, takes the form

$$\frac{\partial h'}{\partial t} + \mu \left(u^* \frac{\partial h'}{\partial x} + v^* \frac{\partial h'}{\partial y} \right) + \omega \left(\frac{\partial h'}{\partial p} + \frac{1-K}{p} h' \right) = Q_h + F_h \quad (4)$$

for each of the nine layers of the model, $K = R/C_p$, R being the gas constant and C_p the specific heat at constant pressure. F_h represents the horizontal diffusion of heat and Q_h is the non-adiabatic heating and includes condensation and evaporation, heating from the surface and heating due to sub-grid-scale convection.

The lower boundary condition $W = dz/dt = \mathbf{V} \cdot \nabla H$

at $z = H$, where H is height of the topography, is approximately satisfied by applying it at $p = 1000\text{mb}$; this gives the 1000mb height tendency equation

$$\frac{\partial h_{10}}{\partial t} + \mu \left(u^* \frac{\partial}{\partial x} (h_{10} - H) + v^* \frac{\partial}{\partial y} (h_{10} - H) \right) + \omega \frac{\partial h_{10}}{\partial p} = F_h \quad (5)$$

where h_{10} is the height of the 1000mb surface.

The remaining equation is the water balance equation which is used in the form

$$\frac{\partial r}{\partial t} + \mu \left(u^* \frac{\partial r}{\partial x} + v^* \frac{\partial r}{\partial y} \right) + \omega \frac{\partial r}{\partial p} = W + F_r \quad (6)$$

for the seven moist layers of the model (the model atmosphere is dry above 300mb) where \bar{r} is the mean humidity mixing ratio of the appropriate 100mb slab. F_r represents the horizontal diffusion of water vapour and W is the rate of humidity mixing ratio due to gain or loss due to condensation and evaporation, transfer from the surface and transfer due to sub-grid-scale convection. These equations are solved numerically by the integration scheme described in section 4. For the remainder of this discussion we shall neglect the dissipative, topographic and non-adiabatic effects and also drop the water balance equation (6). It is also convenient to recast the governing equations into a vector form and to this end we define the following ten-dimensional vectors

$$\underline{u} = (u_1^*, u_2^*, \dots, u_{10}^*)^T$$

$$\underline{v} = (v_1^*, v_2^*, \dots, v_{10}^*)^T$$

$$\underline{\omega} = (\omega_1, \omega_2, \dots, \omega_{10})^T$$

$$\underline{h} = (h_1, h_2, \dots, h_{10})^T$$

where $()^T$ means transpose, u_k^* and v_k^* are the horizontal components of velocity in the pressure surface $p = k \times 100\text{mb}$, h_k is the height this surface and ω_k is the vertical velocity at

$$\underline{A} \frac{\partial \underline{h}}{\partial t} + \underline{N}_h + \mu \underline{B} \left(\frac{\partial u}{\partial x} + \frac{\partial v}{\partial y} \right) = 0 \quad (11)$$

With $\underline{B} = \Delta p \underline{\Gamma} (\underline{A}^T)^{-1} \underline{D}$.

An useful alternative form of this equation is

$$\frac{\partial \underline{h}}{\partial t} + \underline{A}^{-1} \underline{N}_h + \frac{\mu}{g} \underline{G} \left(\frac{\partial u}{\partial x} + \frac{\partial v}{\partial y} \right) = 0 \quad (12)$$

where $\underline{G} = g \underline{A}^{-1} \underline{B}$.

3. Pure gravity waves in the 10-level model

The equations governing the motion of small amplitude gravity waves in the model described by equations (7), (8) and (12) are

$$\frac{\partial u}{\partial t} + g \frac{\partial \underline{h}}{\partial x} - f v = 0 \quad (13)$$

$$\frac{\partial v}{\partial t} + g \frac{\partial \underline{h}}{\partial y} + f u = 0 \quad (14)$$

$$\frac{\partial \underline{h}}{\partial t} + \frac{1}{g} \underline{G} \left(\frac{\partial u}{\partial x} + \frac{\partial v}{\partial y} \right) = 0 \quad (15)$$

where we have assumed that $\mu = 1$. For the remainder of this section we shall neglect the coriolis terms and assume that $\underline{G} = \underline{G}_0$ a constant matrix, that is independent of x, y and t , corresponding to the standard ICAO values of the $\underline{\Gamma}_k$ ($k = 1, 2, \dots, 10$). With these approximations the elimination of u and v between equations (13), (14) and (15) gives the following 'vector' wave equation for \underline{h}

$$\frac{\partial^2 h}{\partial t^2} - \underline{G}_0 \nabla^2 h = 0, \tag{16}$$

where $\nabla^2 \equiv \frac{\partial^2}{\partial x^2} + \frac{\partial^2}{\partial y^2}$.

This equation has normal or Fourier mode solutions

$$h = \underline{\hat{Y}} \text{EXP}(i(\alpha x + \beta y - \sigma t))$$

where the amplitude $\underline{\hat{Y}}$

satisfies the equation

$$\left(\underline{G}_0 - c^2 \underline{I} \right) \underline{\hat{Y}} = 0 \tag{17}$$

and $c = \sigma / (\alpha^2 + \beta^2)^{1/2}$ is the phase speed of this normal mode and \underline{I} is the identity matrix. For given α and β equation (17) is an algebraic eigenvalue problem with real positive eigenvalues c^2 and eigenfunctions $\underline{\hat{Y}}$. There are ten distinct solutions $(c_{0,k}^2, \underline{\hat{Y}}_k)$, $k = 1, 2, \dots, 10$, where $c_{0,k}$ is the phase speed of the normal mode with vertical structure $\underline{\hat{Y}}_k$. The suffix 0 indicates the association between these eigenvalues $c_{0,k}^2$ and the ICAO matrix \underline{G}_0 . If we order the $c_{0,k}$ such that $c_{0,k} > c_{0,k+1}$ then $(c_{0,1}, \underline{\hat{Y}}_1)$ corresponds to the external mode and $(c_{0,k}, \underline{\hat{Y}}_k), k \neq 1$, to the k th internal mode. The ten wave-speeds for the ICAO standard atmosphere are given in Table 1.

The matrix $\underline{E} = (\underline{\hat{Y}}_1, \underline{\hat{Y}}_2, \dots, \underline{\hat{Y}}_{10})$ has the property that $\underline{E}^{-1} \underline{G}_0 \underline{E} = \underline{C}_0^2 = \text{diag}(c_{0,1}^2, c_{0,2}^2, \dots, c_{0,10}^2)$ and we can use this relation to decouple the system of equations (13), (14) and (15) into ten subsystems each subsystem describing the evolution of one of the models gravity waves. This decoupling is achieved by a change of dependent variables and we define new 'velocities' \underline{a} and \underline{b} and 'heights' \underline{Y} by the transformations

MARGIN

CLASSIFICATION

-No-

MAX TYPING AREA

CLASSIFICATION

(8)

$$\left. \begin{aligned} \underline{a} &= \underline{E}^{-1} \underline{u} \\ \underline{b} &= \underline{E}^{-1} \underline{v} \\ \underline{Y} &= \underline{E}^{-1} \underline{h} \end{aligned} \right\} \quad (18)$$

On substituting for \underline{u} , \underline{v} and \underline{h} from (18) into equations (13), (14) and (15) we get the ten scalar systems

$$\left. \begin{aligned} \frac{\partial a_k}{\partial t} + g \frac{\partial Y_k}{\partial x} &= 0 \\ \frac{\partial b_k}{\partial t} + g \frac{\partial Y_k}{\partial y} &= 0 \\ \frac{\partial Y_k}{\partial t} + \frac{c_k^2}{g} \left(\frac{\partial a_k}{\partial x} + \frac{\partial b_k}{\partial y} \right) &= 0 \end{aligned} \right\} \quad k = 1, 2, \dots, 10 \quad (19)$$

and we are quite at liberty to integrate each subsystem differently.

Explicit schemes such as the leap-frog scheme and the Lax-Wendroff scheme for the equations in (19) are stable provided the time-step, τ , between time levels satisfies

$$\tau < \Delta x / (\sqrt{2} c_{0,k}) \quad k = 1, 2, \dots, 10$$

In the fine mesh rectangle version of the 10-level model, with a 100km grid length, this amounts to a maximum time-step of three minutes with

$c_{0,1} = 300 \text{ ms}^{-1}$. Unconditionally stable implicit schemes can be used for each subsystem necessitating the solution of ten Helmholtz equations, but because $c_{0,3} \approx 55 \text{ ms}^{-1}$ it is possible to treat two of the subsystems implicitly ($k = 1, 2$) and the remaining eight explicitly and still take a time-step of about 20 minutes. Robert et al's (1972) scheme amounts to an implicit treatment of equations (13), (14) and (15) which generates a three-dimensional Helmholtz equation.

a) The integration scheme for (19)

New values of the dependent variables at time level $(n+1)$,
 $(t = t_0 + (n+1)\tau)$ where τ is the time-step and t_0
 the initial time, are obtained using the implicit scheme

$$\left. \begin{aligned} a_k^{n+1} &= a_k^n - \frac{\tau}{2} g \left(\frac{\partial Y_k^n}{\partial x} + \frac{\partial Y_k^{n+1}}{\partial x} \right) \\ b_k^{n+1} &= b_k^n - \frac{\tau}{2} g \left(\frac{\partial Y_k^n}{\partial y} + \frac{\partial Y_k^{n+1}}{\partial y} \right) \\ Y_k^{n+1} &= Y_k^n - \frac{\tau}{2} \frac{C_{0,k}^2}{g} \left(\left(\frac{\partial a_k}{\partial x} + \frac{\partial b_k}{\partial y} \right)^n + \left(\frac{\partial a_k}{\partial x} + \frac{\partial b_k}{\partial y} \right)^{n+1} \right) \end{aligned} \right\} (20)$$

for the external and first internal modes, $k = 1, 2$ and
 the explicit scheme

$$\left. \begin{aligned} a_k^{n+1} &= a_k^n - \tau g \frac{\partial Y_k^{n+1}}{\partial x} \\ b_k^{n+1} &= b_k^n - \tau g \frac{\partial Y_k^{n+1}}{\partial y} \\ Y_k^{n+1} &= Y_k^n - \frac{\tau C_{0,k}^2}{g} \left(\frac{\partial a_k}{\partial x} + \frac{\partial b_k}{\partial y} \right)^n \end{aligned} \right\} (21)$$

for the remaining modes, $k = 3, 4, \dots, 10$. The implicit
 scheme (20) is unconditionally stable whilst the explicit scheme
 (21) is stable provided

$$\tau < \min_k \left(\Delta x / (\sqrt{2} C_{0,k}) \right) = \Delta x / (\sqrt{2} C_{0,3}).$$

Eliminating a_k^{n+1} and b_k^{n+1} in (20) gives

$$Y_k^{n+1} = Y_k^n - \frac{\tau C_{o,k}^2}{g} \left(\frac{\partial a_k}{\partial x} + \frac{\partial b_k}{\partial y} \right)^n + \left(\frac{\tau}{2} \right)^2 C_{o,k}^2 \nabla^2 (Y_k^{n+1} + Y_k^n), \quad (k=1,2).$$

If we define $\Psi_k = Y_k^{n+1} + Y_k^n$ then

$$-\left(\frac{\tau}{2} \right)^2 C_{o,k}^2 \nabla^2 \Psi_k + \Psi_k = f_k$$

where $f_k = Y_k^n - \frac{\tau C_{o,k}^2}{g} \left(\frac{\partial a_k}{\partial x} + \frac{\partial b_k}{\partial y} \right)^n + Y_k^n$ } $k = 1, 2. (22)$

Once Ψ_k ($k = 1, 2$) has been determined from (22) with appropriate boundary conditions, we obtain Y_k^{n+1} from

$$Y_k^{n+1} = \Psi_k - Y_k^n = Y_k^n - \frac{\tau C_{o,k}^2}{g} \left(\frac{\partial a_k}{\partial x} + \frac{\partial b_k}{\partial y} \right)^n + (\Psi_k - f_k), \quad (23)$$

that is Y_k^{n+1} is given by the explicit forward time-step of the scheme in (21) plus a correction term and we can write

$$\underline{Y}^{n+1} = \underline{Y}^n - \frac{\tau}{g} \underline{C}_o^2 \left(\frac{\partial \underline{a}}{\partial x} + \frac{\partial \underline{b}}{\partial y} \right)^n + (\Psi_1 - f_1) \underline{e}_1 + (\Psi_2 - f_2) \underline{e}_2 \quad (24)$$

where $\underline{e}_1 = (1, 0, \dots, 0)^T$ and $\underline{e}_2 = (0, 1, 0, \dots, 0)^T$.

Multiplying this equation by \underline{E} gives

$$\begin{aligned} \underline{h}^{n+1} &= \underline{h}^n - \frac{\tau}{g} \underline{C}_o^2 \left(\frac{\partial \underline{u}}{\partial x} + \frac{\partial \underline{v}}{\partial y} \right)^n + (\Psi_1 - f_1) \hat{\underline{y}}_1 + (\Psi_2 - f_2) \hat{\underline{y}}_2 \\ &= \underline{h}^* + (\Psi_1 - f_1) \hat{\underline{y}}_1 + (\Psi_2 - f_2) \hat{\underline{y}}_2 \end{aligned} \quad (25)$$

The computations to produce \underline{h}^{n+1} are performed in the following order

- (i) \underline{h}^* is produced by a forward time-step

(ii) compute f_1 and f_2 , $f_k = \hat{X}_k^T \cdot \left(\frac{h^*}{\tau} + \frac{h^n}{\tau} \right)$
 where \hat{X}_k^T is the k th row of \underline{E}^{-1} and f_k

can also be used as an accurate first guess for

ψ_k , $k = 1, 2$, in the iterative procedure

used to solve the Helmholtz equations (22).

(iii) Solve (22) for ψ_1 and ψ_2 .

(iv) Adjust h^* according to (25) to give h^{n+1}

Finally, it is easy to show that u^{n+1} and v^{n+1} are given by

$$u^{n+1} = u^n - \tau g \frac{\partial h^{n+1}}{\partial x} - \frac{\tau g}{2} \left(2 \frac{\partial \psi_1^n}{\partial x} - \frac{\partial \psi_1}{\partial x} \right) \hat{Y}_1 - \frac{\tau g}{2} \left(2 \frac{\partial \psi_2^n}{\partial x} - \frac{\partial \psi_2}{\partial x} \right) \hat{Y}_2 \quad (26)$$

and

$$v^{n+1} = v^n - \tau g \frac{\partial h^{n+1}}{\partial y} - \frac{\tau g}{2} \left(2 \frac{\partial \psi_1^n}{\partial y} - \frac{\partial \psi_1}{\partial y} \right) \hat{Y}_1 - \frac{\tau g}{2} \left(2 \frac{\partial \psi_2^n}{\partial y} - \frac{\partial \psi_2}{\partial y} \right) \hat{Y}_2 \quad (27)$$

4. The semi-implicit algorithm

The model equations (7), (8) and (11) are integrated in two stages, accomplished by 'splitting' the time rate of change of the dependent variables into two parts, a technique pioneered by Russian meteorologists particularly Marchuk (see Marchuk et al (1968)). The two stages of the integration cycle that produces forecast values at time level $(n+1)$, ($t = t_0 + (n+1)\tau$) where τ is the time-step, from values at time level n are: -

(i) the advection stage

Here we integrate forward a single time-step, τ , the equations

$$\frac{\partial u}{\partial t} + \frac{N_x}{\tau} = 0$$

(12)

$$\left(\frac{\partial v}{\partial t}\right)_N + \frac{N_y}{\Delta t} = 0$$

$$\frac{\Delta}{\Delta t} \left(\frac{\partial h}{\partial t}\right)_N + \frac{N_h}{\Delta t} = 0$$

where $(\partial u / \partial t)_N$ means the time rate of change of u due to the non-linear term N_x with similar interpretations for $(\partial v / \partial t)_N$ and $(\partial h / \partial t)_N$, using the two-step Lax-Wendroff scheme used by Bushby and Timpson (1967) with the grid arrangements shown in Figures 2(a) and 2(b). Thus we obtain temporary values of \hat{u}^{n+1} , \hat{v}^{n+1} and \hat{h}^{n+1} where \hat{u}^{n+1} is given by

$$\underline{u}^{n+1/2} = \underline{u}^n + \frac{\tau}{2} \left(\frac{\partial u}{\partial t}\right)_N^n$$

$$\hat{u}^{n+1} = \underline{u}^n + \tau \left(\frac{\partial u}{\partial t}\right)_N^{n+1/2}$$

with similar expressions for \hat{v}^{n+1} and \hat{h}^{n+1} . Simple centred differences/used for space derivatives except at boundaries where one-sided differences are used;

(ii) the linear adjustment stage

These temporary values \hat{u}^{n+1} , \hat{v}^{n+1} and \hat{h}^{n+1} are now used as initial conditions for a single time-step, τ , integration of the equations

$$\left(\frac{\partial u}{\partial t}\right) + g \frac{\partial h}{\partial x} - f v = 0$$

$$\left(\frac{\partial v}{\partial t}\right) + g \frac{\partial h}{\partial y} + f u = 0$$

$$\left(\frac{\partial h}{\partial t}\right) + \frac{u}{g} \frac{\partial}{\partial x} \left(\frac{\partial u}{\partial x} + \frac{\partial v}{\partial y}\right) = 0$$

using a variant of the scheme described in section 3 which allows for explicit treatment of the coriolis terms and the difference ($\underline{G} - \underline{G}_0$). The grid used for this stage is the one in Figure 2(a). Again simple centred differences are used for the space derivatives. The split semi-implicit scheme is stable provided the time-step τ satisfies the criteria.

$$\left. \begin{aligned} \tau &< \frac{\Delta x}{\sqrt{\mu}} / (|V|_{\max}) && \text{arising from the advection stage} \\ \tau &< \frac{\Delta x}{\sqrt{\mu}} / (\sqrt{2} C_{0,3}) && \\ \text{and if } (C_1 - C_{0,1}) > 0, \tau &< \frac{\Delta x}{\sqrt{\mu}} / (\sqrt{2} (C_1 - C_{0,1})) && \text{arising from the linear adjustment stage} \end{aligned} \right\} \quad (28)$$

where C_1 is the 'local' speed of the external gravity wave corresponding to the variable matrix \underline{G} . The value of $|V|_{\max}$ allowed for is 100 ms^{-1} whilst $C_{0,3} \approx 55 \text{ ms}^{-1}$ and $\max(C_1 - C_{0,1}) \approx 30 \text{ ms}^{-1}$ if $C_{0,1}$ is the ICAO value corresponding to the \underline{G}_0 for the ICAO atmosphere.

5. Discussion

The semi-implicit scheme described in section 4 has been modified to include the moisture equation (6) and the effect of friction and diffusion, topography, surface heating and condensation and evaporation of rain which is forecast by the model. The incorporation and parameterisation of these physical effects are summarised in Benwell et al (1971) for the explicit version of the model. The fine mesh rectangle version of the 10-level model with a 100km horizontal mesh length is integrated using the semi-implicit scheme with a 12 minute time-step compared with a $2\frac{1}{2}$ minute time-step used with Bushby and Timpson's explicit scheme, a factor of 4.8 increase in the time-step. This gives an overall increase in efficiency of about 4.4, some extra work being needed to prepare the right hand sides of the Helmholtz equations and to solve these equations. The quality of the fine

mesh forecasts using the semi-implicit scheme with this increased time-step has not depreciated, in fact on many occasions the semi-implicit scheme gives better results, particularly for developing depressions, than the explicit scheme. This may be due to the different horizontal grid arrangements used by the two schemes resulting in a more accurate evaluation of $\partial h / \partial x$ and $\partial h / \partial y$ with the semi-implicit scheme.

The semi-implicit scheme has been used routinely to produce forecasts on the 64 x 48 grid point (number of height points) fine mesh rectangle area since March 13th 1973. The scheme has recently been coded for the 300km coarse mesh octagon forecast area that covers most of the Northern hemisphere and has been successfully run on two winter cases.

MAXIMUM AREA FOR 31 x 51 - A4

MAXIMUM AREA FOR 31 x 51 - A4

CLASSIFICATION

-No-

CLASSIFICATION

MARGIN

-No-

References

Benwell, G. R. R., Gadd, A. J., Keers, J. F., Timpson, Margaret S., & White, P. W.,
1971 Scientific Paper No. 32 HMSO.

Bushby, F. H. & Timpson, Margaret S., 1967 Q.J. R. Met Soc. 93, pp1-17.

Bushby, F. H. & Whitlam, Clare J., 1961 Q.J. R. Met. Soc. 87, pp374-392.

Eliassen, A., 1956 Sci. Rep. 4, Contract AF 19(604)-1286.

Marchuk, G. I., Vorobiov, V. P., Dymnikov, V. P., & Kontarev, G. R., 1968
Proc. WMO/IUGG Symp. Num. Wea. Pred. Tokyo: Japan Met. Agency.

Robert, A., Henderson, J., & Turnbull, C., 1972 MWR 100 No. 5 pp329-335.

MAX TYPING AREA FOR 8 1/2 x 11 - A4

MAX TYPING AREA FOR 8 1/2 x 5 1/2 - A5

CLASSIFICATION

CLASSIFICATION

MARGIN

-No-

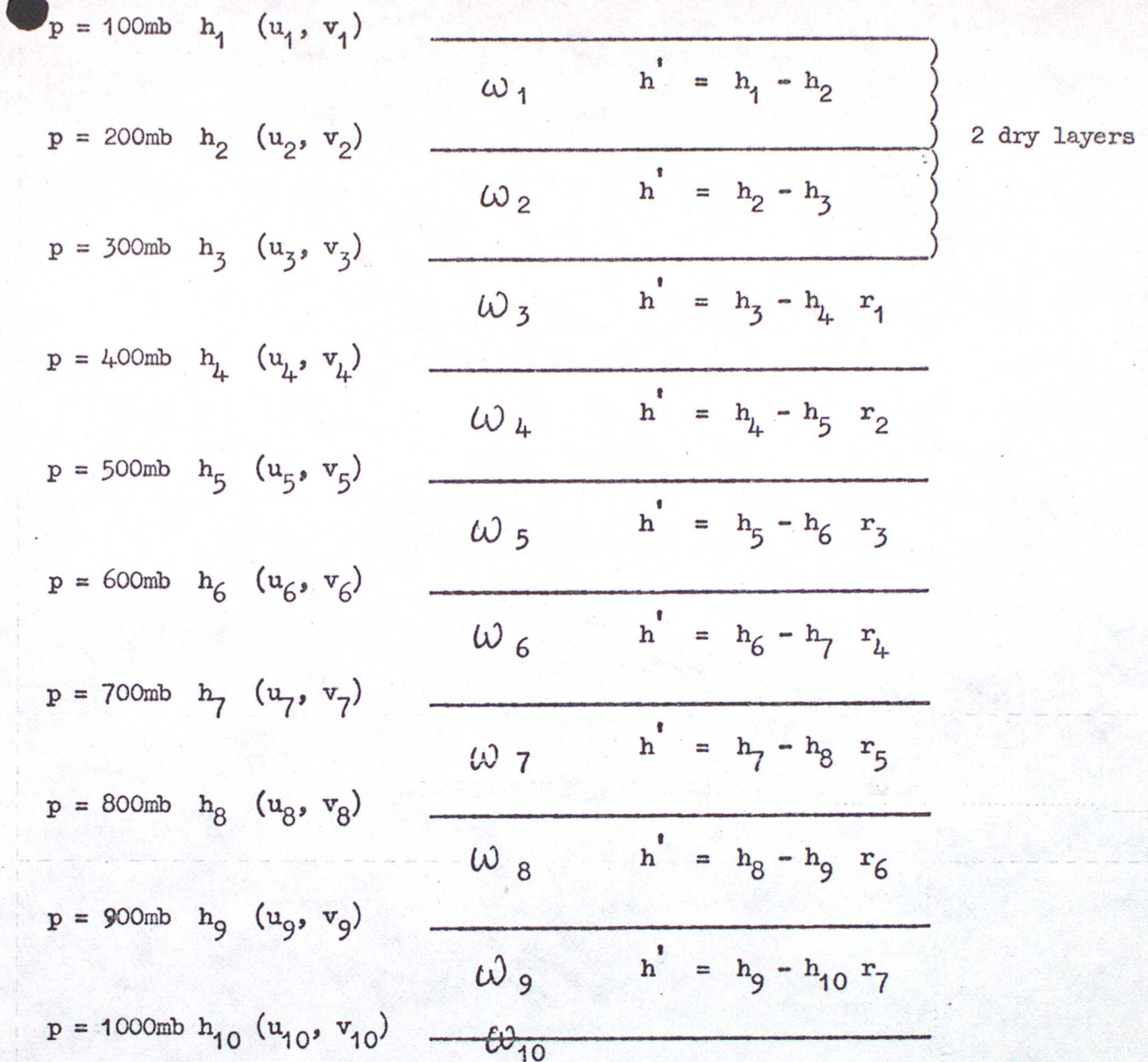


Figure 1. A schematic diagram showing the vertical arrangement of the model's dependent variables.

	v									
h	w	u	hw	u	hw	u	hw	u	hw	u
	v		v		v		v		v	
h	w	u	hw	u	hw	u	hw	u	hw	u
	v		v		v		v		v	
h	w	u	hw	u	hw	u	hw	u	hw	u

(a) Initially and after each complete cycle of the two-step Lax-Wendroff scheme.

	u									
	v		v		v		v		v	
u	hw	u								
	v		v		v		v		v	
u	hw	u								
	v		v		v		v		v	

(b) At intermediate time, that is at the end of the first step of the Lax-Wendroff scheme

Figure 2. Horizontal arrangement of data

k	$C_{g,k}$
1	302 m s ⁻¹
2	115 m s ⁻¹
3	55 m s ⁻¹
4	37 m s ⁻¹
5	23 m s ⁻¹
6	16 m s ⁻¹
7	12 m s ⁻¹
8	9 m s ⁻¹
9	7 m s ⁻¹
10	5 m s ⁻¹

Table 1. The ten phase speeds of the model's gravity waves for an ICAO atmosphere

MAX TYPING AREA FOR 31 x 11 IN. PAPER

MAX TYPING AREA FOR 31 x 11 IN. PAPER

CLASSIFICATION

CLASSIFICATION

MARGIN

-No-